Structure of $Na_{3-3x}Al_xPO_4$, $x = 0$ to 0.5

W. A. DOLLASE*

Department of Earth & Space Sciences, University of California, Los Angeles, California, and Bayerisches Geoinstitut, Universität Bayreuth, Bayreuth, Federal Republic of Germany

AND L. H. MERWIN AND A. SEBALD

Bayerisches Geoinstitut, Universität Bayreuth, Bayreuth, Federal Republic of Germany

Substitution of Al^{3+} and two vacancies for $3Na^+$ in orientationally disordered trisodium phosphate is investigated by multinuclear solid-state MAS NMR and X-ray powder diffraction. ^{27}Al spectra indicate Al on regular tetrahedral sites forming 4 Al–O–P linkages per atom. ^{31}P spectra show a discrete set of resonances assigned to phosphorus forming 0, 1, or 2 P–O–Al linkages. The relative intensities of these resonances indicate that, rather than random, Al is distributed to minimize the number of P–O–Al linkages formed per P atom. Powder X-ray refinements in space group $Fm3m$ indicate that Al, Na, and about 20% of the vacancies are distributed over the $\frac{1}{4}$, $\frac{1}{4}$, $\frac{1}{4}$ sites with the remaining Na and ca. 80% of the vacancies on the $\frac{1}{2}$, 0,0 sites. The orientationally disordered oxygens are well approximated by four partially occupied sites. With increasing Al substitution, PO_4 orientations which "point" along $\langle 100 \rangle$ (toward vacancies and Na atoms) become less common while orientations which point more toward Al and Na at $\frac{1}{4}$, $\frac{1}{4}$, $\frac{1}{4}$ become more common. © 1989 Academic Press, Inc.

Introduction

Orientationally disordered crystals (ODCs) are characterized by the presence of a tightly bonded group (e.g., NH_4^+, CN^-, NO_3^-, SO_4^{2-}) present at normal crystallographic sites but able to adopt any of several (two to innumerable) different orientations (*1*). Such materials are in many respects intermediate between the normal crystalline and the liquid (or amorphous) states and commonly show anomalous thermal, mechanical, and transport properties.

The presence of several possible orientations results in a range of local configurations (interatomic distances, angles, coordination numbers). As conventional diffraction methods yield only the average structure (superposition of all orientations) interpretation of local arrangements generally requires additional data.

Na_3PO_4 belongs to a large family of ODCs which includes the phosphates, arsenates, vanadates, niobates, tantalates, and other tetrahedral oxyanions of most alkali metals, monovalent Ag, and Tl (*2*). The crystal structure of these compounds at temperatures above their transformation

* To whom correspondence should be addressed.

from orientationally ordered phases is particularly simple. They belong to space group $Fm3m$ with TO_4 groups at the origin and face centers of a small cubic unit cell ($a = 7\text{--}8$ Å). The TO_4 groups are therefore in cubic close-packing resulting in two types of intergroup sites: "octahedral" sites (e.g., at $\frac{1}{2}$, 0, 0) with six nearest-neighbor TO_4 groups and "tetrahedral" sites (e.g., at $\frac{1}{4}$, $\frac{1}{4}$, $\frac{1}{4}$) with four nearest-neighbor TO_4 groups. There are one octahedral and two tetrahedral sites per TO_4 group, all occupied by the monovalent ions, yielding the stoichiometry, M_3TO_4. Related families of ODCs with low-valent ions only in the tetrahedral sites (such as Li_2SO_4) or only in the octahedral sites (such as $KClO_4$) and still others (such as CBr_4) with neither site occupied are known (1).

Though the terms "octahedral" and "tetrahedral" refer to the number and arrangement of nearest TO_4 groups, the actual number of bonds formed between a metal atom in one of these sites and the surrounding oxygens depends upon the relative orientations of the (six or four) TO_4 groups surrounding the site. If a TO_4 group has one of its vertices pointing directly at a site, a short, strong M–O bond is formed while if an edge (or face) of the TO_4 group is presented to this site, 2 (or 3) longer and weaker M–O bonds are formed. For some atoms the longest distances may exceed plausible bond lengths. Thus there is a wide range of possible coordination numbers for metal atoms in either site (ideally 0 to 18 for an octahedral-site atom and 0 to 12 for a tetrahedral-site atom).

A further anomalous aspect of ODCs is the wide range of solid solutions commonly formed with ions of disparate size and/or valence. Solid solutions of Na_3PO_4 in which the sodium atoms are extensively replaced with Ca, Zn, Al, Zr, or other atoms (and the requisite number of vacancies to maintain overall charge balance) have been reported (3). In the case of aluminum, up to ca. 1.5 (out of 3) of the moderately large, monovalent Na ions may be replaced by up to ca. 0.5 of the much smaller, trivalent Al ion per formula unit (4).

Crystal structure analyses of orientationally disordered Na_3PO_4 (5, 6), $Na_{2.925}Al_{0.025}PO_4$, and $Na_{2.4}Al_{0.2}PO_4$ (7) have been reported. At zero or small Al content, these studies confirm the arrangement described above including high thermal and/or positional disorder. Although the PO_4 groups are distributed over many orientations, these studies suggest that one of the PO_4 vertices points along $\langle 100 \rangle$ axes (see individual studies for details). The study of the higher Al content sample concluded that the vacancies are restricted to the octahedral sites.

However, the sites, actual coordination numbers, local geometry, and other aspects of the distribution of replacement ions in these solid solutions are generally unknown. Because Al substitution is extensive and amenable to study using both NMR and X-ray techniques, the $Na_{3-3x}Al_x PO_4$ series was selected for further structural investigation.

Experimental Methods

Endmember Na_3PO_4 was synthesized by heating reagent grade $Na_3PO_4 \cdot 10\text{--}12H_2O$ to 400°C. Syntheses starting from Na_2CO_3 + $NH_4H_2PO_4$ showed evidence of loss of Na_2O vapor on heating and were discarded. Na_3PO_4 is polymorphous with the cubic ODC phase stable above ca. 300°C and an ordered, lower-symmetry phase stable at lower temperatures (8). X-ray patterns show, however, that samples cooled rapidly from above 300°C usually contain a mixture of both phases. $AlPO_4$, which is also polymorphous, was synthesized by heating a mixture of $NH_4H_2PO_4$ + $\gamma\text{-}Al_2O_3$ to 1000°C. The X-ray powder diffraction pattern of this sample showed only the $C222_1$ low-cristobalite like polymorph.

Intermediate members of the solid solution were synthesized at approximately 10-mol% intervals (exact compositions are given in Table I) from either the previously prepared $AlPO_4$ + hydrated Na_3PO_4 or the hydrated Na_3PO_4 + $NH_4H_2PO_4$ + Al_2O_3. Mixtures were heated at 800°C (or 750°C for samples with more than 40 mol% $AlPO_4$) for about 20 hr. X-ray powder diffraction patterns show all samples to be well crystallized and to consist almost entirely of the cubic phase. As previously reported, the addition of more than about 5 mol% Al either drops the transition temperature below room temperature or makes the rate of transition more sluggish and allows quenching (4).

Examination of the optical properties using polarized-light microscopy, inspection of very long counting-time diffraction patterns, and in a few cases, the ^{27}Al NMR spectra revealed the presence of potentially significant amounts of impurities in some samples. (Previous studies of these compounds report similar difficulties with impurities (4, 7).) Several of the lowest Al-content samples showed evidence (from X-ray and NMR data) of a sodium aluminate phase (probably Na_5AlO_4) whose presence may be related to the minor excess Na (less than 2.5 wt% expressed as NaOH) present

in reagent grade hydrated Na_3PO_4. These samples were discarded and the syntheses and tests repeated. Any remaining impurity level (estimated as less than 2%) is not expected to influence any of the results reported here.

The ca. 50-mol% $AlPO_4$ sample shows substantial additional X-ray peaks, peak splitting, and weak optical birefringence indicating that it is, at least in part, noncubic. This is consistent with prior studies (4, 7) suggesting that the limit of the cubic solid solution is near this Al content.

High-resolution, solid-state ^{27}Al and ^{31}P NMR spectra were measured on Na_3PO_4, $AlPO_4$, and samples of intermediate composition. The spectra were obtained on a Bruker MSL-300 spectrometer operating at a field of 7 T. Magic-angle spinning (MAS) was achieved by the use of a standard Bruker multinuclear double-bearing probe system. The MAS rotors were constructed of ZrO_2. The ^{27}Al and ^{31}P frequencies were 78.206 and 121.498 MHz, respectively. The ^{31}P spectra were obtained using magic-angle spinning at a rate of ca. 3.5 kHz. All ^{31}P spectra were run with 2-μsec 36° pulse, a recycle delay of 20 sec and 16 transients. The ^{27}Al spectra were obtained in single-pulse mode using a 2-μsec $\pi/6$ pulse, a 10-sec recycle delay, MAS rates of ca. 4 kHz, and from 48 to 144 transients. Where necessary, center bands were assigned by rerunning the ^{31}P MAS spectra at a different MAS rate.

The high-frequency-positive convention is used in the reporting of chemical shifts. Phosphorus-31 shifts were indirectly referenced to 85% aqueous phosphoric acid (H_3PO_4). The secondary reference used was brushite, $CaHPO_4 \cdot 2H_2O$, the shift of which was determined to be 1.2 ± 0.1 ppm by replacement with the standard. Aluminum-27 shifts have been referenced to aqueous $AlCl_3$ by replacement of the sample with the standard. The reported ^{27}Al shifts are the resonance maxima uncor-

TABLE I

NMR SPECTRAL PARAMETERS OF ^{27}Al IN $Na_{3-3x}Al_xPO_4$

x	δ_{exp}^a (ppm)	$\nu_{1/2}^b$ (Hz)
0.09	49	1610
0.19	41	1620
0.29	42	1170
0.38	45	1030
0.43	46	1020
1.00	41	250

^{a} Shifts are relative to Al in aqueous chloride solution, uncorrected for quadrupolar interaction.
^{b} Half-height linewidth.

rected for the effects of quadrupolar inter-action.

X-ray powder data were obtained using Co$K\alpha_1$ radiation on a Stoe diffractometer equipped with a curved-crystal Ge mono-chromator operating in transmission geom-etry and employing a position sensitive de-tector. In the cubic system, with this small cell dimension, all peaks are sufficiently isolated (or exactly superposed) so that in-tegrated intensities can be measured by computer peak fitting of the (background subtracted) raw data. A so-called Lorent-zian-squared peak shape adequately fit the observed data. Intensities were corrected for Lorentz, polarization, monochromator, and absorption effects.

Crystal structures were refined by least-squares fitting of the structural variables to observed intensities, or, for exactly over-lapped reflections, to sums of intensities (9). Using CoKα radiation there are 19 to 21 independent X-ray powder peaks measur-able representing 23 to 25 reflections. The only positional variables are the locations of the disordered oxygen atoms. Their dis-tribution was approximated by adjusting the occupancies of four fixed oxygen posi-tions, with P–O distance of 1.54 Å, along $\langle 001 \rangle$, $\langle 113 \rangle$, $\langle 111 \rangle$, and $\langle 110 \rangle$ directions. This choice of sites, when reproduced by the *Fm3m* symmetry, provides a roughly equally spaced sampling of the sphere. The sum of the oxygen occupancies is con-strained to 16 atoms per unit cell. In addi-tion, the distribution of sodium between oc-tahedral and tetrahedral sites, a scale factor, and two isotropic temperature fac-tors were refined. This simple model closely reproduces the observed intensi-ties. The amount and quality of the X-ray data do not warrant more sophisticated treatment. To check reproducibility, X-ray intensities were remeasured for two com-positions using a second sample or another part of the same sample. In both cases the resulting refined parameters agreed

with the prior determinations within 1 to 2 SD.

Results

^{27}Al NMR Spectra

^{27}Aluminum spectra (example in Fig. 1a) show fairly symmetric single resonances at shifts (uncorrected for quadrupolar interac-tion) given in Table I. For AlPO$_4$ the ob-served shift is in agreement with the uncor-rected value of 39.8 ppm at 6.4 T (corrected value is 42.5 ppm) previously reported for low-cristobalite type AlPO$_4$ (*10*). From the crystal structure (*11*) this resonance can be assigned to AlO$_4$ tetrahedra sharing all four corners with PO$_4$ groups. In each of the solid-solution compositions the resonance maximum retains approximately this same shift. As the only oxygens in this solid solu-tion are those of PO$_4$ groups, all resonances correspond to Al forming 4 Al–O–P link-ages and the near constancy of shift is thus not surprising.

Resonance half-height linewidths (in-cluded in Table I) are markedly broadened relative to (orientationally ordered) AlPO$_4$. These widths may reflect a range of Al–O–P angles and/or Al–O bond lengths due to the orientational disorder of the PO$_4$ groups. The greater width at lower Al con-tents is consistent with a greater orienta-tional freedom of the PO$_4$ groups for which further evidence is given below.

The symmetric, single resonance max-ima, as well as the low intensity of the spin-ning sidebands (Fig. 1a), are qualitatively consistent with a small quadrupole coupling constant and a symmetric site. Together with evidence provided by the chemcial shift, these observations allow unambigu-ous assignment of the Al atoms to the $\frac{1}{4}, \frac{1}{4}, \frac{1}{4}$ sites which have (average) $\overline{4}3m$ symmetry in these cubic compounds. The chemical shift rules out sixfold coordination and Al in the $\frac{1}{2}$, 0, 0 sites coordinated by only four
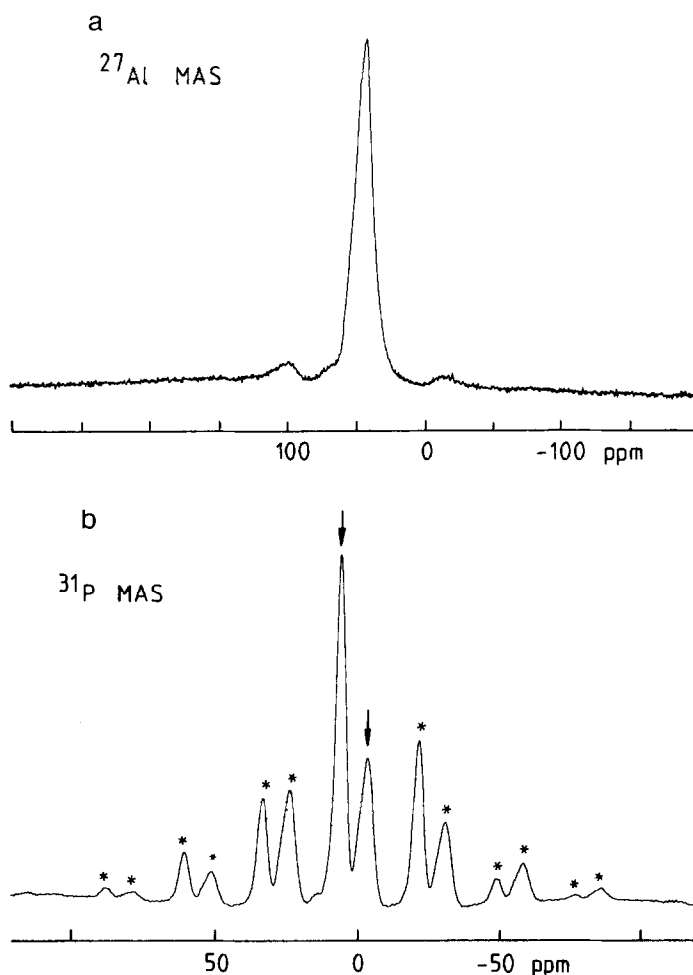
Fig. 1(a). ^{27}Al MAS NMR spectrum $Na_{2.13}Al_{0.29}PO_4$, spinning rate 4.1 kHz, 100 transients. (b) ^{31}P MAS NMR spectrum of $Na_{1.86}Al_{0.38}PO_4$, spinning rate 3.3 kHz, 16 transients. Center bands are indicated by arrows, while asterisks denote spinning side bands.

oxygens would not result in a near isotropic environment.

^{31}P NMR Spectra

^{31}P NMR chemical shifts of the low temperature, low symmetry Na_3PO_4 polymorph and of a mixture of the low and ODC Na_3PO_4 polymorphs are included in Table II. The apparent linewidth of the mixture is only slightly larger suggesting that the chemical shifts and peak breadths of the two polymorphs are closely similar. This chemical shift is near the value of +11.7 ppm previously reported (12) for K_3PO_4, which is isostructural with cubic Na_3PO_4. These high frequency shifts, and the isotropic shielding tensor observed in the potassium compound (12), are consistent with a picture of isolated PO_4 groups weakly bonded to a near isotropic array of large, monovalent ions.

The ^{31}P spectrum of $AlPO_4$ contains a single narrow peak whose parameters (Table

TABLE II

CHEMICAL SHIFTS[a] OF ^{31}P^{nAl} RESONANCES IN Na$_{3-3x}$Al$_x$PO$_4$

x	P^{0Al}	P^{1Al}	P^{2Al}	P^{3Al}	P^{4Al}	$v^b_{1/2}$ (Hz)
0.0[c]	13.8					110
0.0[d]	13.7					150
0.09	13.3	6.1				300, 550
0.19	13.4	5.4				320, 630
0.29	13.4	5.3	−4.9			300, 565, 570
0.38		5.4	−3.9			500, 670
0.43		5.4	−3.8			480, 750
—				(−15)[e]		
1.00					−26.3	275

[a] Referenced to 85% H$_3$PO$_4$.
[b] Widths at half-height of resonance.
[c] Low-temperature form.
[d] Mixture of low-temperature and cubic forms.
[e] Estimated by interpolation.

II) are in good agreement with previously reported "low cristobalite" AlPO$_4$ values at −27.1 ppm, $v_{1/2}$ = 310 Hz (10). This chemical shift, in accord with the known crystal structure (11), indicates PO$_4$ tetrahedra sharing all four corners with AlO$_4$ tetrahedra.

NMR resonances of intermediate members of the solid solution (Table II) are in-

termediate between those of Na$_3$PO$_4$ and AlPO$_4$. However, rather than a continuous change with composition, a series of well-separated, discrete peaks are observed (example in Fig. 1b). Areas under each peak (and associated spinning sidebands) are given in Table III. This systematic set of peaks may be assigned, in analogous fashion, to the well-known concept of ^{29}Si Q-

TABLE III

INTENSITIES[a] OF ^{31}P^{nAl} PEAKS IN Na$_{3-3x}$Al$_x$PO$_4$

x	P^{0Al}	P^{1Al}	P^{2Al}	P^{3Al}	P^{4Al}	x^b_{cal}
0.0	1.0					0.0
0.09	0.81	0.19	—	—	—	0.05
	0.69	*0.27*	*0.04*			
0.19	0.40	0.60	—	—	—	0.15
	0.43	*0.40*	*0.14*	*0.02*		
0.29	0.06	0.85	0.09	—	—	0.26
	0.25	*0.42*	*0.25*	*0.05*	*0.01*	
0.38	0.01	0.56	0.43	—	—	0.36
	0.15	*0.36*	*0.33*	*0.14*	*0.02*	
0.43	—	0.38	0.62	—	—	0.40
	0.11	*0.32*	*0.36*	*0.18*	*0.03*	
1.0					1.0	1.0

Note. Expected values for randomly distributed Al are shown in italic type.
[a] Integrated over respective spinning sideband manifold.
[b] Calculated from $\frac{1}{4}\Sigma n I^{nAl}$.

species (13), to P linked to 0, 1, or 2 Al atoms (denoted herein by P^{0Al}, P^{1Al} . . .). Replacing Na neighbors with the more strongly bonding Al's produces an upfield change in the chemical shift of about 8 to 9 ppm for each additional Al neighbor increasing to about 10 to 11 ppm at highest Al contents. The peaks assigned to each local configuration have about the same chemical shift for all compounds for which they appear. The approximate location of the here unobserved P^{3Al} resonance is estimated by interpolation.

The breadths of individual P^{nAl} resonances (Table II) are roughly constant but broaden as n increases from 0 to 2. This broadening probably reflects the range of Al plus vacancy distributions surrounding the PO_4 groups including $^{31}P-^{27}Al$ dipole interactions. For the P^{0Al} resonance these different arrangements or interactions involve only more distant Al atoms and/or vacancies and this peak is noticeably narrower than the P^{1Al} and P^{2Al} resonances. In these latter configurations additional broadening relative to the P^{0Al} resonance, as well as the P^{4Al} resonance of orientationally ordered $AlPO_4$, may reflect a variability of P–O–Al angles (10).

The relative intensities of the spinning sidebands are relatively small for the P^{0Al} resonance and increase with an increase in the number of Al next-nearest neighbors (Fig. 1b). This is best interpreted as an increase in the anisotropy of the ^{31}P shielding tensor as the number of P–O–Al linkages per PO_4 group increases from 0 to 2.

X-ray

The results of the X-ray crystal structure analyses of the solid solution members are given in Table IV. Refinement of sodium site occupancies indicates about 20% of the vacancies occur on tetrahedral sites and about 80% on octahedral sites, qualitatively consistent with neutron powder diffraction data (7). Al atoms are assigned to the tetra-

hedral sites on the basis of the NMR data, but there is so little difference between the X-ray scattering of Al and Na that any interchange would make no difference in the fit of the X-ray data. A high degree of disorder, represented by high values of the "temperature" factors, is found at all compositions and is in agreement with the previous powder neutron diffraction studies (6, 7).

Because of the orientational disorder, the X-ray data do not directly furnish meaningful interatomic distances, angles, or coordination numbers. However, a change in the average PO_4 orientation with composition is clearly observed. With increasing substitution of Al on the tetrahedral sites, and removal of Na from the octahedral sites, there is a systematic decrease of oxygen density in the $\langle 100 \rangle$ direction and an increase in the $\langle 113 \rangle$ and $\langle 111 \rangle$ directions. That is, as Al with its stronger (shorter) bonding requirements increases on the tetrahedral sites, the PO_4 groups increasingly adopt orientations with P–O bonds "pointing" toward, or more nearly toward, the tetrahedral sites, and less commonly toward the decreasing number of sodiums in the octahedral sites.

Conclusions

Na_3PO_4 in its face-centered cubic form contains orientationally disordered PO_4 groups. Each PO_4 is surrounded by a cube of 8 Na^+ ions on tetrahedral sites and, slightly further, by an octahedron of 6 Na^+ ions on octahedral sites. In order to form bonds of sufficient strength to the more remote octahedral Na's and avoid what would be too short (too strong) bonds to tetrahedral Na's, PO_4 tetrahedra must have a fairly high likelihood of one or more of their corners pointing approximately along $\langle 100 \rangle$ directions and very little probability of pointing along $\langle 111 \rangle$ directions. Such PO_4

TABLE IV

RESULTS OF X-RAY CRYSTAL STRUCTURE ANALYSES: $Na_{3-3x}Al_xPO_4$, SPACE GROUP = $Fm3m$,
4 FORMULA UNITS PER UNIT CELL

| Atom | #/cell | Fixed Parameters | | | |
		x	y	z	B^a
P	4	0	0	0	g
Al	$4x$	.25	.25	.25	g
Na^{vi}	b	.5	.5	.5	h
Na^{iv}	$12-12x-b$	.25	.25	.25	g
O(1)	c	.00	.00	.208	g
O(2)	d	.063	.063	.188	g
O(3)	e	.120	.120	.120	g
O(4)	f	.147	.147	.000	g

| | Variable Parameters | | | | |
	$x = 0.09$	$x = 0.19$	$x = 0.29$	$x = 0.38$	$x = 0.43$
a = cell^b	7.411(1)	7.412(1)	7.404(1)	7.396(1)	7.394(1)
b = Na^{vi}	3.4(2)	2.8(2)	2.2(2)	1.4(2)	1.2(1)
c = O(1)	5.7(4)	3.9(4)	2.5(4)	0.8(4)	0.6(4)
d = O(2)	6.1(4)	7.6(4)	7.6(4)	10.6(4)	9.6(4)
e = O(3)	0.3(4)	0.7(4)	0.8(4)	1.6(4)	1.7(4)
f = O(4)	3.9(4)	3.8(4)	5.1(4)	3.0(4)	4.1(4)
g = B	4.8(2)	4.7(1)	4.9(1)	4.9(1)	5.7(1)
h = $B(Na^{vi})$	10(1)	10(1)	11(1)	12(2)	12(2)
R-factor	4.7%	3.0%	3.7%	6.4%	6.4%

^{a} Isotropic temperature factor in $Å^2$.

^{b} Cell dimension in $Å$.

orientations are entirely consistent with the previously published crystal structures.

The orientational disorder, or more precisely the orientational freedom, of the PO_4 groups allows extensive replacement of sodium by aluminum atoms plus charge-balancing vacancies. ^{27}Al NMR spectra indicate that aluminums replace sodiums on tetrahedral sites while X-ray data show the vacancies predominantly replace sodiums on the octahedral sites.

Considerations of tetrahedral Al–oxygen bond lengths show that when a Na atom is replaced by an Al, it is necessary for the surrounding PO_4 groups to turn a vertex more toward (though probably not directly at) a $\langle 111 \rangle$ direction. In so doing, the PO_4 group vertex can no longer point at the Na atoms in the octahedral sites. This is where the vacancies come in. Their contribution to the free energy of this structure is to replace, preferentially, the octahedral Na atoms. It is probable that the vacancies and Al replacements are therefore spatially correlated rather than independently (randomly) distributed.

^{31}P NMR spectra show discrete resonances for P atoms forming 0, 1, or 2 P–O–Al linkages. The areas under the ^{31}P NMR resonance peaks give the relative numbers of phosphorus atoms in each configuration. The total number of P–O–Al linkages obtained from the sum of the products of the peak areas times the number of Al linkages associated with each peak must equal the number of Al–O–P linkages per formula unit, $Na_{3-3x}Al_xPO_4$. With Al in tetrahedral coordination by oxygen and all oxygens be-

longing to PO_4 groups this latter value is $4x$, i.e.,

$$\Sigma n I^{nAl} = 4x, \qquad (1)$$

where I^{nAl} is the normalized fractional intensity of the P^{nAl} resonance. The compositions derived from the NMR peak areas therefore provide an independent test of the peak assignment model. Comparison of ideal synthesis compositions with those derived from the NMR peak areas (Table III) shows fairly close agreement although the compositions derived from the NMR data are consistently 2–4 mol% lower than those calculated from reactant proportions.

The relative proportions of the various P^{nAl} configurations do not correspond to a purely random distribution (Table III, italic entries). In particular, at each composition, phosphorus atoms forming higher numbers of P–O–Al linkages are strongly suppressed relative to a random distribution. Thus with increasing Al content, essentially all P's form one P–O–Al linkage before any form two P–O–Al linkages and so on. As a result only one or two configurations have appreciable populations at any composition.

The presence of several Al neighbors further restricts PO_4 orientation making it increasingly difficult for the remaining oxygen corners to form bonds of appropriate length to their Na atom neighbors. This is probably why the Al distribution tends to avoid, insofar as possible, higher P–O–Al linkages. Though these data are insufficient to prove such a distribution, the P^{nAl} intensities approximately correspond with what would be seen if the Al atoms tend to keep as far apart from each other as is possible. Similar maximum Al dispersion in aluminosilicates has been postulated from ^{29}Si NMR spectra (13).

The increasing restriction of PO_4 orientation with increasing Al content may be expected to ultimately reduce those properties characteristic of orientationally disordered crystals. This is consistent with the observations that at Al contents beyond about 20 to 30% the melting temperature and high ionic conductivity decrease (4).

With maximum Al dispersion, 50 mol% Al corresponds to all PO_4 groups forming two P–O–Al linkages. Previous studies (4, 7) report that near this composition, and certainly at higher Al contents, low-temperature glasses or noncubic crystalline phases are obtained. In this study, a sample with 48 mol% Al shows optical and X-ray evidence of a noncubic phase. ^{31}P NMR spectra of this sample show a weak P^{1Al} resonance and a strong P^{2Al} resonance (at their appropriate chemical shifts) plus additional, narrower resonances evidently due to a second, and probably more ordered, phase. It may be that PO_4 groups with more than two P–O–Al linkages are energetically proscribed in the ODC structure and perhaps that $Na_3Al(PO_4)_2$ (that is, $x = 0.5$) is an ordered compound of lower symmetry.

Acknowledgments

References

1. N. G. PARSONAGE AND L. A. STAVELY, "Disorder in Crystals," Chap. 7, Clarendon Press, Oxford (1978).
2. G. MEYER AND R. HOPPE, Rev. Chim. Min. 12, 454 (1975).
3. J. T. IRVINE AND A. R. WEST, J. Solid State Chem. 74, 385 (1988).
4. A. HOOPER, P. MCGEEHIN, K. T. HARRISON, AND B. C. TOFIELD, J. Solid State Chem. 24, 265 (1978).
5. D. M. WIENCH AND M. JANSEN, Z. Anorg. Allg. Chem. 461, 101 (1980).
6. J. M. NEWSAM, A. K. CHEETHAM, AND B. C. TOFIELD, Solid State Ionics 1, 377 (1980).
7. J. M. NEWSAM, A. K. CHEETHAM, AND B. C. TOFIELD, Solid State Ionics 1, 395 (1980).

8. M. PALAZZI AND F. REMY, *Bull. Soc. Chim. Fr.* **8**, 2795 (1971).

9. M. J. COOPER, K. D. ROUSE, AND M. SAKATA, *Z. Kristallogr.* **157**, 101 (1981).

10. D. MÜLLER, E. JAHN, G. LADWIG, AND U. HAUBENREISSER, *Chem. Phys. Lett.* **109**, 332 (1984).

11. R. C. MOONEY, *Acta Crystallogr.* **9**, 728 (1956).

12. A. R. GRIMMER AND U. HAUBENREISSER, *Chem Phys. Lett.* **99**, 487 (1983).

13. G. ENGELHARDT AND D. MICHEL, "High-Resolution Solid-State NMR of Silicates and Zeolites," p. 181, Wiley, Chichester (1987).